The Initial-Value Problem of Spherically Symmetric Wyman Sector Nonsymmetric Gravitational Theory

M. A. Clayton,
CERN-Theory Division, CH-1211 Geneva 23, Switzerland

L. Demopoulos, and J. Légaré
Department of Physics, University of Toronto, Toronto, Ontario, Canada M5S 1A7

(March 22, 1997)

We cast the four-dimensional field equations of the Nonsymmetric Gravitational Theory (NGT) into a form appropriate for numerical study. In doing so, we have restricted ourselves to spherically symmetric spacetimes, and we have kept only the Wyman sector of the theory. We investigate the well-posedness of the initial-value problem of NGT for a particular data set consisting of a pulse in the antisymmetric field on an asymptotically flat space background. We include some analytic results on the solvability of the initial-value problem which allow us to place limits on the regions of the parameter space where the initial-value problem is solvable. These results are confirmed by numerically solving the constraints.

I. INTRODUCTION

Of late, there has been an increasing interest in numerical relativity and the application of numerical techniques to the study of dynamical gravitational objects. The reason for this is fairly clear: numerical relativity makes it possible to study physical situations that have defied analytic analysis.

The Nonsymmetric Gravitational Theory (NGT) (see [1–6], as well as [7] for the most recent discussion) is an alternate theory of gravity that evolved from a re-interpretation of the Einstein Unified Field Theory (UFT) (see [8–15]), itself an extension of Einstein's General Relativity (GR). The theory proposes to do away with the assumption that the metric tensor describing spacetime is a symmetric, second-rank tensor, replacing it with a second-rank, nonsymmetric tensor. This tensor is typically written as the metric tensor in GR: $g_{\mu\nu}$. However, since a metric tensor is by definition a symmetric quantity, $g_{\mu\nu}$ cannot represent the metric of the NGT spacetime; instead, we refer to it as the fundamental tensor (see the discussion in [10–12] and in particular [14]).

Although on the surface the above-mentioned substitution appears innocuous, in reality it induces fundamental changes in the underlying structure of the theory, both physical and mathematical. Indeed, because of the lack of a definite tensorial symmetry in the various quantities of the theory, the field equations of NGT are somewhat more complicated than the corresponding field equations of GR, as is the dynamical structure. For instance, it can be shown that a spherically symmetric gravitational field in GR is diffeomorphic to a static, spherically symmetric solution, so that all spherically symmetric stellar objects have a static exterior. This is known as Birkhoff's theorem (see for instance [16], p. 372). In contrast, it was demonstrated in [17] that there is no equivalent to Birkhoff's theorem in NGT. Hence, if we wish to study a stellar object even so simple as a spherically symmetric star in NGT, we must consider the full, time-dependent theory.

The increased mathematical complication of the field equations of NGT *versus* those of GR has meant that NGT has been plagued since its inception by a distinct lack of exact, or in some cases even approximate, solutions. In particular, in addition to the (trivial) GR solutions, a single static solution to the spherically symmetric field equations is known to exist for massless NGT: the so-called Wyman solution (see [18–21]). The so-called Papapetrou solution (see [22], in particular §I) has been formally eliminated from the theory (see [7]). The addition of terms to the action by Moffat [4–7] does not simplify matters: exact solutions for the massive theory are even more elusive than for the massless theory. It therefore appears that NGT would be an ideal candidate for numerical investigations.

In this work, we begin the task of defining a formalism that will allow the application of the techniques developed in the field of numerical relativity to NGT; the work was begun in [23–25], where a Hamiltonian formulation of NGT was derived from the action principle of the theory. It was found in these references that the antisymmetric degrees of freedom separate into two sectors, namely the Wyman sector and the Papapetrou sector. One of these sectors, specifically the Papapetrou sector, is plagued with linearization instabilities; this is, in fact, what motivated the work in [7], which eliminates these degrees of freedom. However, since the two sectors of the theory are decoupled in evolution, by choosing Wyman sector initial data, our results are equally applicable to most UFT-like actions.

The next section gives a brief overview of the coordinate choices and slicing conditions that allow us to rewrite the set of first-order field equations in a form appropriate for numerical study. In §III we discuss the initial-value problem, as well as some difficulties that arise when dealing with a constrained set of field equations, in particular how those problems apply to NGT. In §IV we discuss the numerical techniques relevant to the solution of the initial-value problem of NGT. We also present one such generated solution and discuss its properties. The first appendix contains the spherically symmetric reduction of the field quantities, while the second appendix gives the conformal transformation rules of the field equations. The last appendix is a brief demonstration of two results used in §III.

II. THE SPHERICALLY SYMMETRIC NGT FIELD EQUATIONS

Early versions of NGT [1–3] consisted of a re-interpretation of UFT, where the antisymmetric components of the fundamental tensor, originally introduced to represent the components of the electromagnetic field, were considered gravitational degrees of freedom. The work in [26,27] necessitated the addition of two terms to the action. One of these, the so-called Bonnor term (see [28]), endowed the antisymmetric fields with a mass and introduced a parameter μ into the theory. This parameter is referred to interchangeably as the NGT mass parameter or the inverse of the NGT range parameter. The findings of [25] lead to a further modification of the theory, described in [7]. This left μ as a free parameter of the theory, with a potential phenomenological interpretation in applications such as galaxy dynamics (see [29]).

Rather than re-iterating the full set of four dimensional NGT field equations here, we will simply refer the interested reader to the literature (see, for instance, [1–7], [17], and [23], among others). Instead, we offer in Appendices A and B an overview of the spherically symmetric, Wyman sector field equations written in first-order form; these will be sufficient for our purposes. These appendices serve also to define the notation we use in this work. The goal of the current section is to make the coordinate choices and to choose the slicing conditions that will reduce the NGT field equations to a form amenable to numerical study.

Upon performing a conformal transformation of the field variables: $\gamma^{ab} \to \phi^{-4}\gamma^{ab}$ and $K_{ab} \to \phi^{-2}K_{ab}$, where γ^{ab} is the inverse of the hypersurface metric and K_{ab} is its extrinsic curvature (for details, see Appendix B), we find that, just as in GR, the Hamiltonian and momentum constraints remain inter-twined. In order to make any headway in solving these constraints, we must find a way of decoupling them. In GR, this is accomplished, for example, by using maximal slicing: $\mathrm{Tr}[K] = K^{\mu}{}_{\nu} = \gamma^{\mu\nu}K_{\mu\nu} = 0$, which fully decouples the Hamiltonian and momentum constraints. Preserving this condition in time, $\partial_t[\mathrm{Tr}[K]] = 0$, yields a second-order elliptic equation for the lapse function: $\gamma^{ab}\nabla_a\nabla_b[N] - NR^{(3)} = 0$ (see, for instance, (3.4) in §III.B of [30]). A similar approach can be taken in NGT; however, the resulting "lapse equation" is not nearly as simple as its GR counterpart. Instead, it turns out to be more profitable to take[1] $K^2{}_2 = 0$. In this case, the symmetric-sector components of the extrinsic curvature drop out completely from the Hamiltonian constraint. Although both the conformal factor and the extrinsic curvature still appear in the momentum constraint, it is only the K_{11} component of the latter that appears. Therefore, if a solution to the Hamiltonian constraint can be found, this can be inserted into the momentum constraint, which can then be solved for the remaining component of the extrinsic curvature.

In spherical symmetry, there is only one coordinate choice to be made: a radial coordinate r is chosen such that $[(\gamma^{22})^2 + (\gamma^{[23]})^2]^{1/2} = R^{-2}(r)$, where $R(r)$ is some currently unspecified function; we will choose $R(r) = r$. This choice can obviously be satisfied by taking $\gamma^{22} = R^{-2}(r)\cos\psi$ and $\gamma^{[23]} = R^{-2}(r)\sin\psi$, or $\tan\psi = \gamma^{[23]}/\gamma^{22}$. The components of the surface Ricci tensor are then (see Appendix A)

$$
\begin{aligned}
R^{\mathrm{NS}(3)}_{11} &= -2\partial_r^2[\ln R] - 2(\partial_r[\ln R])^2 - \tfrac{1}{2}(\partial_r[\psi])^2 - \partial_r[\ln\gamma^{11}]\partial_r[\ln R], \\
R^{\mathrm{NS}(3)}_{22} &= 1 - R^2\gamma^{11}(\cos\psi\partial_r^2[\ln R] - 2\cos\psi(\partial_r[\ln R])^2 - \tfrac{1}{2}\sin\psi\partial_r^2[\psi] - \sin\psi\partial_r[\ln R]\partial_r[\psi]) \\
&\qquad - \tfrac{1}{2}R^2\partial_r[\gamma^{11}](\cos\psi\partial_r[\ln R] + \tfrac{1}{2}\sin\psi\partial_r[\psi]),
\end{aligned}
$$

and

$$
\begin{aligned}
R^{\mathrm{NS}(3)}_{[23]} &= -R^2\gamma^{11}(\sin\psi\partial_r^2[\ln R] - 2\sin\psi(\partial_r[\ln R])^2 + \tfrac{1}{2}\cos\psi\partial_r^2[\psi] + \cos\psi\partial_r[\ln R]\partial_r[\psi]) \\
&\qquad - \tfrac{1}{2}R^2\partial_r[\gamma^{11}](\sin\psi\partial_r[\ln R] - \tfrac{1}{2}\cos\psi\partial_r[\psi]),
\end{aligned}
$$

from which the Ricci scalar is found to be

---

[1]From Appendix A, $K^2{}_2 = \gamma^{22}K_{22} + \gamma^{[23]}j_{[23]}$ and $j^2{}_3 = \gamma^{[23]}K_{22} - \gamma^{22}j_{[23]}$.

$$R^{\mathrm{NS}(3)} = -2\gamma^{11}(2\partial_r^2[\ln R] + 3(\partial_r[\ln R])^2) + 2R^{-2}\cos\psi - \tfrac{1}{2}\gamma^{11}(\partial_r[\psi])^2 - 2\partial_r[\gamma^{11}]\partial_r[\ln R]. \tag{1}$$

We also define

$$R^2{}_2 = \gamma^{22}R^{\mathrm{NS}(3)}_{22} + \gamma^{[23]}R^{\mathrm{NS}(3)}_{[23]} = R^{-2}\cos\psi - \gamma^{11}\partial_r^2[\ln R] - 2\gamma^{11}(\partial_r[\ln R])^2 - \tfrac{1}{2}\partial_r[\gamma^{11}]\partial_r[\ln R],$$

and

$$R^2{}_3 = \gamma^{[23]}R^{\mathrm{NS}(3)}_{22} - \gamma^{22}R^{\mathrm{NS}(3)}_{[23]} = R^{-2}\sin\psi - \tfrac{1}{2}\gamma^{11}\partial_r^2[\psi] - \gamma^{11}\partial_r[\ln R]\partial_r[\psi] - \tfrac{1}{4}\partial_r[\gamma^{11}]\partial_r[\psi].$$

As mentioned above, if we choose the slicing condition $K^2{}_2 = 0$, the Hamiltonian and momentum constraints are effectively decoupled, allowing them to be solved independently.[2] In fact, using the definition of the derivative operator $\Delta_\gamma[\,]$ given in (C1), the Hamiltonian constraint is written

$$\mathcal{H} = 0 = [\gamma^{11}]^{-1/2}\phi[8\Delta_\gamma[\phi] - \phi R^{\mathrm{NS}(3)} + 2R^2\phi^{-7}[(j^2{}_3)^2 - K^2{}_2(K^2{}_2 + 2K^1{}_1)] + \tfrac{1}{4}\mu^2R^2\phi^5\sin^2\psi] \tag{2a}$$

$$= [\gamma^{11}]^{-1/2}\phi[8R^2\gamma^{11}\partial_r^2[\phi] + 16R\gamma^{11}\partial_r[\phi] + 4R^2\partial_r[\phi]\partial_r[\gamma^{11}] + \tfrac{1}{2}R^2\phi\gamma^{11}(\partial_r[\psi])^2 + 2R\phi\partial_r[\gamma^{11}] - 2\phi\cos\psi + 2\phi\gamma^{11} + 2R^2(j^2{}_3)^2\phi^{-7} + \tfrac{1}{4}\mu^2R^2\phi^5\sin^2\psi], \tag{2b}$$

while the momentum constraint becomes $\mathcal{H}_1 = -2R^2[\gamma^{11}]^{-1/2}(\gamma^{11}K_{11}\partial_r[\ln(R^2\phi^4)] - j^2{}_3\partial_r[\psi]) = 0$. The latter one of these is solved for the sole remaining symmetric-sector component of the extrinsic curvature in a straightforward manner:

$$K_{11} = \frac{j^2{}_3\partial_r[\psi]}{\gamma^{11}\partial_r[\ln(R^2\phi^4)]}. \tag{3}$$

That the momentum constraint can be solved for K_{11} in this fashion allows us to implement a "semi-constrained" evolution. What is more, by setting $\phi = 1$ in (2b), we obtain a first-order, ordinary differential equation for γ^{11}, whose solution on every time-slice would generate the evolution of that field variable. This would allow us to implement a fully constrained evolution, eliminating both the Hamiltonian and momentum constraints, as well as the symmetric-sector evolution equations, hence by-passing the problems inherent in evolving a set of discretized field equations (see, for instance, the discussion of the Cauchy problem in [31], as well as the issues raised in [32] and [33] on the maintenance of constraints during numerical evolution). However, at this time there does not seem to be any obvious advantage in doing this, and it would only further cloud the issue of the solvability of the Hamiltonian constraint (see §III below). In this work, we have chosen to implement the semi-constrained evolution mentioned above.

Naturally, the slicing condition $K^2{}_2 = 0$ and the coordinate choice $[(\gamma^{22})^2 + (\gamma^{[23]})^2]^{1/2} = R^{-2}(r)$ mentioned above must be enforced: $\partial_t[K^2{}_2] = 0$ and $\partial_t[R] = 0$. The first of these leads to an equation for the lapse function:

$$\frac{\partial_r[N]}{N} = -\frac{R}{\gamma^{11}\partial_r[R\phi^2]}[\gamma^{11}\partial_r^2[\phi^2] + R^{-6}\phi\partial_r[\phi]\partial_r[\gamma^{11}R^6] + \tfrac{1}{4}\mu^2\phi^6\sin^2\psi]. \tag{4}$$

This first-order, ordinary differential equation is solved on every time-slice for the lapse function. Meanwhile, preserving the coordinate condition in time leads to an equation for the only non-trivial component of the shift function:

$$\partial_r[N^1] - 2N^1\partial_r[\ln(R\phi^2)] - 2N\phi^{-6}K^2{}_2 = 0. \tag{5}$$

When $K^2{}_2 = 0$, the solution of this is $N^1 = AR^2\phi^4$, where $A(t)$ is a constant of integration; here, we take $A(t) = 0$, so that $N^1 \to 0$ as $r \to +\infty$, maintaining asymptotically flat spatial slices in evolution.

Once the slicing conditions, coordinate choices, and constraints are taken care of, the evolution equations are:

$$\partial_t[\gamma^{11}] = -2N\phi^{-6}[\gamma^{11}]^2K_{11} \tag{6a}$$

$$\partial_t[\psi] = 2N\phi^{-6}j^2{}_3 \tag{6b}$$

$$\partial_t[K_{11}] = 4N[\phi\partial_r^2[\phi] - (\partial_r[\phi])^2] + 2\phi\partial_r[\phi](N\partial_r[\ln\gamma^{11}] + 2N\partial_n[\ln R] - \partial_r[N]) + \phi^2\partial_r^2[N] + \tfrac{1}{2}\phi^2\partial_r[N]\partial_r[\ln\gamma^{11}] - N\phi^2R^{\mathrm{NS}(3)}_{11} + N\phi^{-6}\gamma^{11}[K_{11}]^2 + \tfrac{1}{4}\mu^2N\phi^6[\gamma^{11}]^{-1}\sin^2\psi \tag{6c}$$

$$\partial_t[j^2{}_3] = N\phi\gamma^{11}\partial_r[\phi]\partial_r[\psi] + \tfrac{1}{2}\phi^2\gamma^{11}\partial_r[N]\partial_r[\psi] - N\phi^2R^2{}_3 - N\phi^{-6}\gamma^{11}K_{11}j^2{}_3 - \tfrac{1}{2}\mu^2N\phi^6\sin\psi\cos\psi. \tag{6d}$$

Note that we have included here the evolution equation for K_{11}, for the sake of completeness.

---

[2] Strictly speaking, the Hamiltonian constraint must be solved first, and its solution must be used to solve the momentum constraint.

III. THE INITIAL-VALUE PROBLEM IN NGT FOR SPHERICALLY SYMMETRIC SYSTEMS

In the words of York and Piran, "The initial value problem of a physical theory is ascertaining what data must be specified at a given time in order that the equations of motion determine uniquely the evolution of the system." (see [34], p. 147). In formulating NGT as a Hamiltonian system, Clayton (see [23]) laid most of the groundwork for the study of its initial-value problem. As with most Lagrangian field theories, the field equations of NGT separate into a set of initial-value constraints that impose diffeomorphism invariance, and a set of evolution equations. In this section, we are concerned with the initial-value constraints of NGT, also known as the Hamiltonian and momentum constraints.

It was demonstrated in the previous section that the momentum constraint can be explicitly satisfied, as in (3), and we need not be concerned with it any further. Meanwhile, the Hamiltonian constraint is a second-order, ordinary differential equation for ϕ, the conformal factor. Unlike the momentum constraint, the solvability of the Hamiltonian constraint is by no means guaranteed. Indeed, we can gain some insight by recognizing, as did Wheeler (see [35,36]) the similarity between the Hamiltonian constraint (for a moment of time-symmetry) and a scattering problem in non-relativistic Schrödinger mechanics, with the curvature scalar playing the role of the potential. If $R^{\mathrm{NS}(3)}$ is positive everywhere, then the Hamiltonian will always have a solution, corresponding to scattering off a potential barrier. If the curvature scalar is negative but "shallow" enough, then a scattering solution will also exist. Only if $R^{\mathrm{NS}(3)}$ is negative and "deep" enough will a bound state begin to form, and hence no scattering solution will exist. This is the type of behaviour that will be manifest itself below: there are actually situations where the antisymmetric fields could be considered perturbations on a GR background, in the sense that they are by no means large, in which the Hamiltonian constraint has no asymptotically flat solution. Of course, the reason for this behaviour is that the derivatives of the antisymmetric variables enter the curvature scalar, along with the variables themselves. Thus, one can choose values for the antisymmetric variables that are small in overall magnitude, but that are sharply peaked, causing a corresponding "deepening of the well", which in turn causes the Hamiltonian constraint to become unsolvable for an asymptotically flat spacetime.[3]

In Appendix C, we derive two results that are consequences of the existence of a solution to the Hamiltonian constraint, given the appropriate boundary conditions. In other words, the solvability of the Hamiltonian constraint implies that the inequalities (C3) and (C4) are satisfied. However, it is important to keep in mind that these inequalities hold only for massless NGT, when $\mu = 0$. The mass term in (2) makes it considerably more difficult to generate similar inequalities for the case of massive NGT. Furthermore, we emphasize that these inequalities are consequences of the solvability of the Hamiltonian constraint: to demonstrate that these inequalities actually imply that a solution to the Hamiltonian constraint exists is a somewhat more involved process, and will be considered in the future.

Given an initial data set, $\{\gamma^{11}, \psi, {j^2}_3\}$, we can use (C3) to place a limit on the field variables that will allow us to solve the Hamiltonian constraint for an asymptotically flat spacetime. The procedure is actually one of elimination: if we find values of the field variables for which (C3) is not verified, then we may conclude that the Hamiltonian constraint cannot be solved for such an initial data set, as the proof in Appendix C concludes that if the Hamiltonian constraint is solvable, then (C3) is verified.[4] This process is continued, making the initial data set evermore conservative, for instance by moving closer and closer to a Minkowski space initial data set, until (C3) is verified. At this point, we cannot conclude that a solution of the Hamiltonian constraint exists: rather, we conclude that a solution certainly *does not* exist for less conservative initial data.

If this procedure is to help us in placing limits on the solvability of the Hamiltonian constraint, then we require a (non-trivial) function f that makes the left-hand side of (C3) a minimum. This function is well-known [38]: $f(r) = [\xi/(\xi^2 + r^2)]^{1/2}$. Here ξ is a constant, and the factor of $\xi^{1/2}$ in the numerator is included to make the value of the left-hand side of (C3) independent of ξ; (C3) is obviously invariant under such a scaling of f. The value of ξ is then used to make the value of the right-hand side of (C3) as large as possible. Note in particular that the maximum of f occurs at $\xi = \pm r$.

As noted in Appendix C, the two inequalities (C3) and (C4) are used to different ends. We mentioned above that (C3) is used to find a *most* conservative initial data set $\{\gamma^{11}, \psi, {j^2}_3\}$ for which the Hamiltonian constraint is guaranteed to be unsolvable. On the other hand, (C4) is used to find a *least* conservative initial data set for which the Hamiltonian constraint is guaranteed to be solvable. In a sense, the two inequalities, (C3) and (C4) are used to

---

[3] In such a case, a solution would most likely exist for a non-asymptotically flat manifold or a closed manifold (as in [37]); we are not considering that option here.

[4] It is the converse which is not necessarily true: (C3) might very well be verified, yet the Hamiltonian constraint might not possess a solution.

"sandwich" the limiting initial data set where the Hamiltonian constraint is just barely solvable.

In this work, we are considering initial data sets in which $\gamma^{11} = 1$, $j^2{}_3 = 0$, and where ψ has the form of a pulse:

$$\psi(r) = A[r/r_0]^2 e^{-(r-r_0)^2/\sigma^2}. \tag{7}$$

The dimensionless parameter A gives the overall amplitude of the pulse, while r_0 and σ are lengths that fix the position and the width, respectively, of the pulse; the location of the maximum of the pulse is $r_{\rm peak} = \frac{1}{2}[r_0 + [r_0^2 + 4\sigma^2]^{1/2}]$. This particular function was chosen because the Gaussian factor causes both ψ and its derivatives to vanish quite rapidly away from r_0, while the factor of $[r/r_0]^2$ ensures that the Ricci curvature scalar in (1) remains finite as $r \to 0$. In a sense, the pulse is "semi-localized" about $r = r_{\rm peak}$, allowing us to study the properties of NGT initial data without having to worry about this will affect the boundary conditions. For such an initial data set, the curvature scalar is more or less peaked about $r = r_0$. We therefore choose $\xi = r_{\rm peak}$, in order to maximize the value of the integrand, $f^2 R^{\rm NS(3)}$. The remaining three free parameters, A, σ, and r_0, are adjusted in the manner discussed above until the inequality in (C3) is no longer verified. For instance, since taking $A = 0$ reduces the initial data set to that of Minkowski space, then we expect to find some maximum value $A = A_{\rm max}$ which renders the Hamiltonian constraint unsolvable. Of course, this is intuitively obvious: if there is to be a data set for which the Hamiltonian constraint cannot be solved for an asymptotically flat spacetime, then we expect that data set to correspond to a strong-field region. However, as was mentioned above, it is not only the overall scale of the antisymmetric variables that affects the solvability of the Hamiltonian constraint, but also the scale of their derivatives. In particular, smaller values of the width parameter σ will cause ψ to become correspondingly more peaked, and the ensuing increase in its derivative could feasibly make the Hamiltonian constraint unsolvable.

As we approach a region of unsolvability in the parameter space, the mass of the system, as measured by an observer in the asymptotically flat region, begins to increase without bound. This is to be expected: a large value of the mass would arise out of a spacetime of such great curvature that it can no longer be represented by an asymptotically flat manifold. It is therefore of great interest to measure the mass of the system as a function of the parameters of the pulse defining ψ. Through an analysis of the surface terms that arise out of the canonical decomposition of the action [23], it can be shown that the ADM mass (see [39]) for asymptotically flat initial data[5] is

$$M = \bar{M} - \frac{1}{2\pi} \oint_{\partial\Sigma} \gamma^{ab} \nabla_a[\phi]\, dS_b \tag{8}$$

where $\partial\Sigma$ is the boundary of the spatial slice and where $\bar{M}$ is the ADM mass of the conformal metric and M is the ADM mass of the physical metric. For the conformally flat field variables we consider, and given the fall-off that we have assumed, it is a simple matter to demonstrate that (8) reduces to

$$M = -2 \int_0^{+\infty} \Delta_\gamma[\phi]\, r^2 dr \tag{9}$$

where the derivative operator $\Delta_\gamma[\,]$ is defined in (C1). Once a solution to the Hamiltonian constraint is found, it can be inserted into (9), and the mass M calculated; note that this mass is guaranteed to be positive as $R^{\rm NS(3)}$ and the Bonnor term are negative definite. Alternately, if we assume that $\phi \to 1 + M/2r$ asymptotically, where M is a constant, we can read off the value of M by inspecting the behaviour of ϕ in the asymptotic region.

In the next section, we discuss a numerical scheme that can be used to analyze the initial-value problem of NGT. In addition to presenting a typical solution to the Hamiltonian constraint, we use this scheme and the conditions discussed above to place limits on the solvability of the initial-value problem in NGT.

IV. NUMERICAL ANALYSIS OF THE INITIAL-VALUE PROBLEM IN NGT

As written, the Hamiltonian constraint (2b) is a second-order, ordinary differential equation for the conformal factor ϕ. There are two important points to note. Firstly, suppose we choose GR initial conditions: *i.e.*, $\gamma^{11} = 1$, $R = r$ (standard spherical coordinates), and vanishing antisymmetric-sector data ($\psi = 0$ and $j^2{}_3 = 0$). The Hamiltonian constraint then reduces to $r^2\partial_r^2[\phi] + 2r\partial_r[\phi] = \partial_r[r^2\partial_r[\phi]] = 0$, whose solution is $\phi = 1 + M/2r$, where M is a constant

[5] For our purposes, asymptotically flat initial data is defined by the usual conditions on the symmetric-sector functions (as in GR), and "faster" fall-off in the antisymmetric-sector variables. This is defined explicitly in [23], p. 116.

of integration, physically interpreted as being the mass defined by (9). Secondly, when $\mu \neq 0$, the Hamiltonian constraint is a non-linear, second-order, ordinary differential equation for the conformal factor, in contrast to GR, where the Hamiltonian constraint for a vacuum spacetime is linear in the conformal factor when the extrinsic curvature vanishes (moment of time symmetry); to see the non-linear behaviour, matter or energy of some kind must be added to the system. Of course, this non-linearity in the Hamiltonian constraint is a manifestation of the fact that, loosely speaking, the antisymmetric-sector fields behave like matter or energy to the symmetric-sector fields, albeit with a nontrivial interaction. Fortunately, since the Hamiltonian constraint in spherical symmetry is an ordinary differential equation, we can use a fairly simple scheme for its solution, and it is this procedure that we describe in this section.

Since we are considering initial data that are concentrated in an area of the initial slice, in those areas of the initial slice where the initial data of the antisymmetric sector are vanishing or nearly so, ϕ will be more or less approximated by its GR solution, $\phi \approx 1 + M/2r$, where M is either some constant or a linear function of r. The first case corresponds to a Schwarzschild-like region of the initial slice, while the second case is physically equivalent to a flat, Minkowski region of the initial slice.[6] We would expect to find the former behaviour in the asymptotic region, while the latter behaviour would be prominent near the origin, given our choice of ψ. The only region which remains in question is the intermediate region, where the antisymmetric-sector initial data are non-trivial; however, this essentially becomes a region of transition that serves the purpose of matching the Minkowski-type solution near the origin to the Schwarzschild-type solution of the exterior. The obvious generalization is therefore to assume that M no longer has this simple behaviour, and to make the substitution $M \to M(r)$. We will therefore use $\phi(r) = 1 + M(r)/2r$ for all r, and solve the Hamiltonian constraint for the function $M(r)$.

Upon substituting $\phi = 1 + M(r)/2r$ into the Hamiltonian constraint (2b), we obtain

$$\partial_r^2[M] = \frac{\partial_r[\ln\gamma^{11}]}{2r}(M - r\partial_r[M]) + \frac{1}{2}\left[\frac{1}{r}\left(\frac{\cos\psi}{\gamma^{11}} - 1\right) - \partial_r[\ln\gamma^{11}] - \tfrac{1}{4}r(\partial_r[\psi])^2\right]\phi - \frac{r(j^2{}_3)^2}{2\gamma^{11}\phi^7} - \frac{\mu^2 r\phi^5\sin^2\psi}{16\gamma^{11}}, \quad (10)$$

where ϕ is to be considered shorthand for $\phi = 1 + M(r)/2r$. This equation is finite-differenced across the spatial grid, using centred differences for both the first- and second-order derivatives,

$$\partial_r[M] \to \frac{\delta(\mu M)_i}{\delta(\mu r)_i} = \frac{M_{i+1} - M_{i-1}}{2\Delta r} \qquad \text{and} \qquad \partial_r^2[M] \to \frac{\delta}{\delta r_i}\left[\frac{\delta M_i}{\delta r_i}\right]_i = \frac{M_{i+1} - 2M_i + M_{i-1}}{\Delta r},$$

where Δr is the (uniform) spatial grid spacing.[7] This yields an equation of the form $M_{i+1} - 2M_i + M_{i-1} = f(M)$, where the notation $f(M)$ is used to represent the fact that the right-hand side has some functional dependence on the value of M at grid points $i+1$, i, and $i-1$, along with the other variables. An implicit relaxation scheme is used to solve this equation[8]: beginning with an initial guess M_i^0 for the M_i, we write $M_{i+1}^j - 2M_i^j + M_{i-1}^j = f(M^{j-1})$ and solve for the M^j. This process is repeated until a precision criterion is reached: in our case, we chose to calculate the integral of the left and right sides of (10) for a given iteration. If the difference between these two is smaller than some predetermined value, then the solution has converged and the iteration ceases. The accuracy of the results will be discussed at the end of this section.

Evidently, (10) and its finite-differenced counterpart are to be augmented by boundary conditions on M that will fix the exact physical situation that is being studied. In this work, we have chosen to take M to be linear in r near the origin. Numerically, this boundary condition is most easily implemented by noting that if M is linear in r, then the average value of M at a given point coincides with the value of M itself at that point: $(\mu M)_i = M_i$. Evaluating this at the origin, where $M = 0$, we have $(\mu M)_0 = 0$, where we have labeled the origin by gridpoint $i = 0$. In the asymptotic region, we have taken M to behave like a constant, and thus its derivative must vanish: $\partial_r[M] = 0$. This guarantees that $\phi \to 1$ as $r \to +\infty$. Numerically, this is encoded using either a backward difference based on the grid point n, or a forward difference based on the grid point $n-1$, where n labels the outer-most grid point: because the derivative is made to vanish, both formulations are equivalent. Therefore, in the asymptotic region, we take either $(\triangledown M)_n = 0$ or $(\triangle M)_{n-1} = 0$.

In Figure 1, we give a plot of the conformal factor of massless NGT for the initial conditions $\gamma^{11} = 1$ and $j^2{}_3 = 0$, with ψ given by (7) with $A = 0.7$ and $r_0 = 40$ in units where $\sigma = 10$; in this and in every other case in this paper,

---

[6] If M is a linear function of r, then $M/2r$ is some constant, and therefore ϕ is a constant other than unity. However, by rescaling the basis vectors, we can absorb this constant and make $\phi = 1$, just as in the case of Minkowski space.

[7] The notation is standard: see, for instance, [40], p. 48, for definitions of the centred-differencing operator, δ, and the averaging operator, μ, as well as the forward- and backward-differencing operators, $\triangle$ and $\triangledown$, which will be used later.

[8] Such schemes are described in the standard references; see, for instance, [41], p. 86.

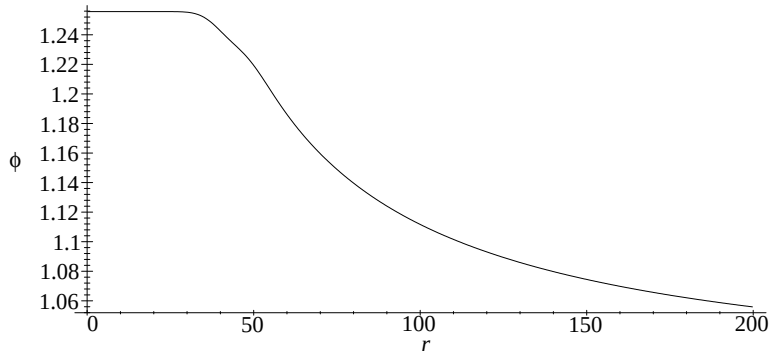

FIG. 1. The conformal factor ϕ of massless NGT as a function of radial distance from the origin, for the initial conditions $\gamma^{11} = 1$, $\psi = A[r/r_0]^2 e^{-(r-r_0)^2/\sigma^2}$, and $j^2{}_3 = 0$. We have taken $A = 0.7$ and $r_0 = 40$ in units where $\sigma = 10$. The radial variable r is measured in the same units as r_0. These data have an ADM mass of $M \approx 22.340$ in the same units as r.

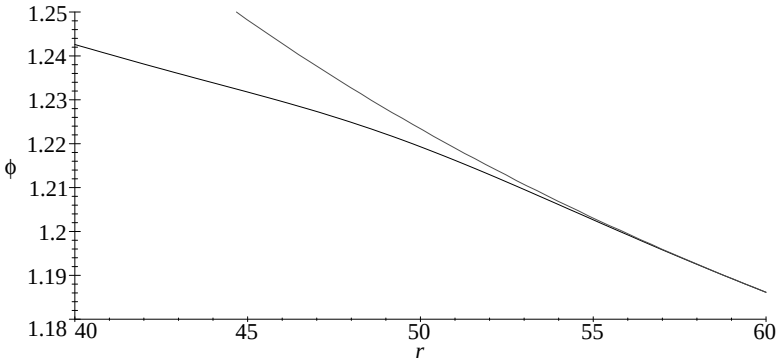

FIG. 2. For the same initial data and parameters as Figure 1, we overlay a magnified region of that graph (lower curve) onto a plot of the GR conformal factor, $1 + M/2r$, where $M \approx 22.340$ in the same units as r.

the units of r, r_0, σ, and M will be assumed to be the same. The solution was found using the implicit relaxation scheme described above. The values of the parameters were chosen to place the simulation in an intermediate region of the parameter space: sufficiently far away from Minkowski space so as to avoid making the simulation trivial, and sufficiently far away from the regions of unsolvability discussed in §III to avoid infringing on some limiting case that could raise questions about the stability of the numerical solution. Throughout, we have chosen $r_{\max}$, the location of the outermost grid point, to be at least $r_{\text{peak}} + 10\sigma$: this guarantees that $\psi(r_{\max}) \approx 0$ and that we can impose asymptotically flat boundary conditions. The grid spacing was taken to be $\Delta r = 0.015$ in the same units as r. In other words, the solution depicted in Figure 1 represents a generic conformal factor for the initial data set used in this work, with the antisymmetric sector variables being strong, but not pathologically so. The ADM mass of the system (see the discussion in §III, in particular (8) and (9) for the definition of the ADM mass in NGT) is calculated to be $M \approx 22.340$. The graph of Figure 2 overlays the GR conformal factor $1 + M/2r$, where $M \approx 22.340$, atop a magnified section of the conformal factor generated from the numerical code. This graph demonstrates that $M(r)$ goes to a constant in the asymptotic region, despite the large width ($\sigma = 10$) of the initial data.

The solution displayed in Figure 1 evidently possesses many of the features described earlier. In fact, the radial axis is clearly divided into three regions, corresponding to the central peak of ψ, and the regions a few widths σ above and below this peak. For our choice of parameters, the central peak of ψ is located at $r_{\text{peak}} \approx 42.36$. The region $0 < r \lesssim 30$ corresponds to a Minkowski space solution, while the region $r \gtrsim 60$ corresponds to a Schwarzschild-type solution, $\phi = 1 + M/2r$, where M is a constant; in this case, $M \approx 22.34$. In the latter region, which is at least two widths away from the central peak at r_{peak}, the value of ψ is, by construction, entirely negligible. The antisymmetric sector field variables behave essentially like an shell of energy to the symmetric sector field variables, which then collapse to their GR form: *i.e.*, Schwarzschild-like. This much is hardly surprising, and indeed, could easily have been predicted based on a perturbative analysis of the Hamiltonian constraint. However, what is somewhat more surprising is how quickly the solution to the Hamiltonian constraint relaxes to its GR form outside the influence of the antisymmetric sector field variables. In fact, it is clear from Figure 2 that in the region $50 \lesssim r \lesssim 60$, ϕ has essentially returned to its GR form: the difference between the two curves in the graph is at its greatest less than 0.5%, and this despite the fact that this region lies within two widths of the central peak of ψ. Indeed, at $r = 50$, $\psi(50)/\psi(r_{\text{peak}}) \approx 0.54$, which is hardly negligible. This demonstrates the rather surprising result that the antisymmetric field variables can very well be non-trivial, and yet the gravitational system as a whole still behaves very much like GR, at least as far as the initial-value problem is concerned.

In Figures 3 through 8 we present plots of the measured mass of the gravitational field versus the various parameters of the pulse; the value of the parameters that remain fixed for the plot are given in the figure caption. For the massless NGT calculations, we also supply in the figure caption the bounds on the parameters determined from (C3) and (C4); note that our initial data allows us to use the flat-space Sobolev constant. Of particular importance is the behaviour of the mass as a function of the pulse width, σ, for the case of massive NGT. We see from Figure 6 that there is a *maximum* value of σ above which the Hamiltonian constraint is no longer solvable. Loosely speaking, this implies that the pulse (7) must be sufficiently small *and* sufficiently peaked (for a given amplitude) in order for a solution to the Hamiltonian constraint to exist. This seems somewhat counter-intuitive; however, when $\mu \neq 0$, we see from (2) that the term proportional to μ^2 contains a factor of $\sin^2\psi$, and is also proportional to ϕ^6. An increasing value of the width causes the factor of $\sin^2\psi$ to become non-trivial in a larger region of the spatial slice, thereby increasing the energy contained in the gravitational system. Consequently, this forces ϕ to stray from its assumed $\phi \to 1$ fall-off, and the Hamiltonian constraint becomes unsolvable. It therefore stands to reason that this highly non-linear term can affect the resulting solution to a great extent. Of course, a similar behaviour can be observed in the abscence of this term: loosely speaking, increasing the width increases the amount of antisymmetric field that is present on the spatial slice, therefore adding to the energy of the system. However, we have found that this occurs at width values on the order of $\sigma \approx 217$, where $M \approx 3190$. The inequalities in Appendix C give $51000 \leqslant \sigma^2 \leqslant 55000$. We conclude that the non-linear term in (2) simply compounds this problem.

We note from the figures that there are clearly defined asymptotes in the mass as a function of the parameter being investigated; these asymptotes correspond to the divergence of the mass as we approach a region of unsolvability of the Hamiltonian constraint in the parameter space. In particular, the mass plots for massless NGT have asymptotes which respect the bounds set by the results of Appendix C. For instance, from Figure 3 we see that the asymptote of the mass as a function of the amplitude lies at $A \approx 0.70$. This compares well with the bounds of $A \geqslant 0.51$ and $A \leqslant 0.81$ set by (C4) and (C3), respectively. Similarly, the asymptote of the mass as a function of the width squared (see Figure 5) lies at about $\sigma^2 \approx 0.005$ for $r_0 = 40$. This is to be compared with the bounds of $\sigma^2 \geqslant 0.0046$ and $\sigma^2 \leqslant 0.090$ obtained from (C3) and (C4), respectively. Finally, the asymptote of the mass as a function of the position of the pulse r_0 (see Figure 7) lies at $r_0 \approx 620$ for $\sigma^2 = 1.6$, in comparison to the values of $r_0 \geqslant 160$ and $r_0 \leqslant 750$ obtained from (C4) and (C3), respectively.

Generically, the asymptotes of the mass are more clearly defined for massless NGT than for massive NGT. This is most pronounced when plotting the mass M versus the position of the pulse r_0: it is clear from Figure 8 that the

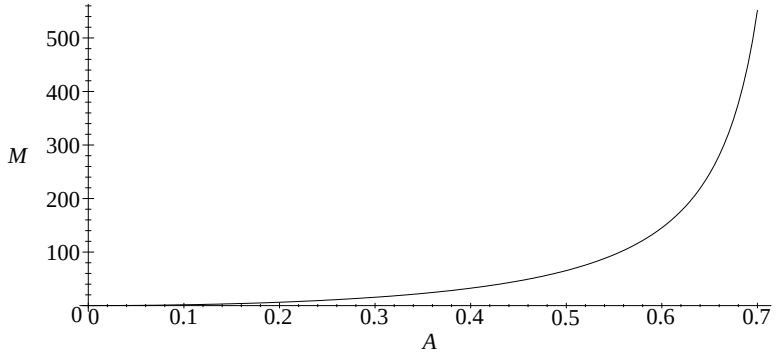

FIG. 3. The mass of the gravitational field versus the amplitude A of the pulse for massless NGT, where $\sigma^2 = 3$ in units where $r_0 = 40$. The inequalities in Appendix C give $0.51 \leqslant A \leqslant 0.81$.

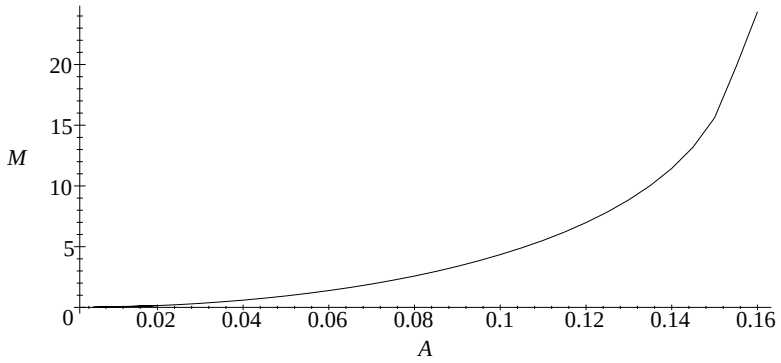

FIG. 4. The mass of the gravitational field versus the amplitude A of the pulse for massive NGT, where $\sigma^2 = 3$ in units where $r_0 = 40$.

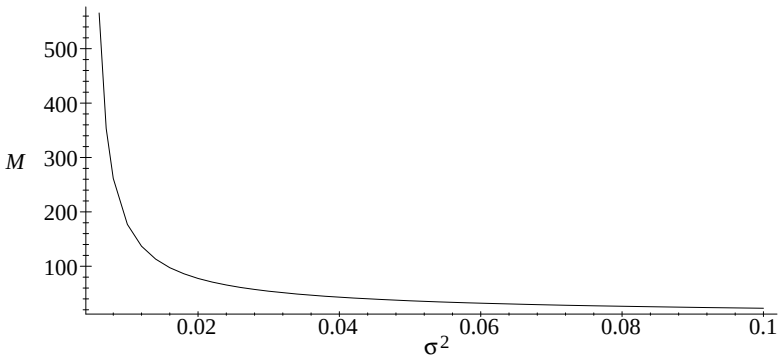

FIG. 5. The mass of the gravitational field versus the squared width σ^2 of the pulse for massless NGT, where $A = 0.15$, and where $r_0 = 40$ in the same units as σ. The inequalities in Appendix C give $0.0046 \leqslant \sigma^2 \leqslant 0.090$ for the left asymptote, in those same units; the leftmost point on the graph is at $\sigma^2 \approx 0.0060$, where $M \approx 566$.

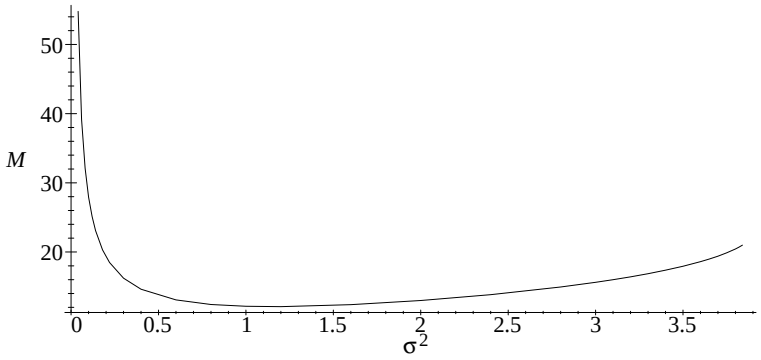

FIG. 6. The mass of the gravitational field versus the squared width σ^2 of the pulse for massive NGT, where $A = 0.15$, and where $r_0 = 40$ in the same units as σ.

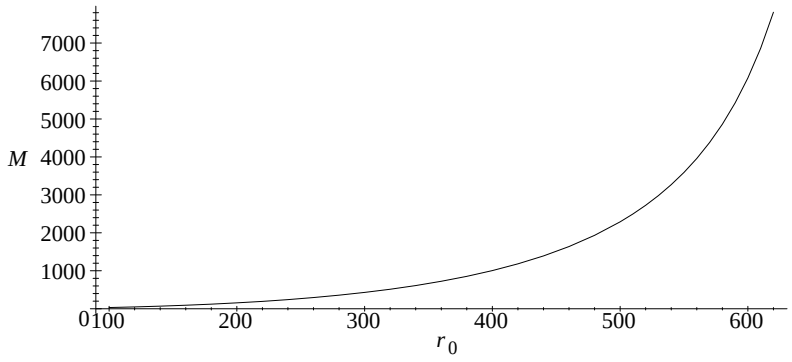

FIG. 7. The mass of the gravitational field versus the position r_0 of the pulse for massless NGT, where $A = 0.15$, and where $\sigma^2 = 1.6$ in the same units as r_0. The inequalities in Appendix C give $160 \leqslant r_0 \leqslant 750$ in those same units.

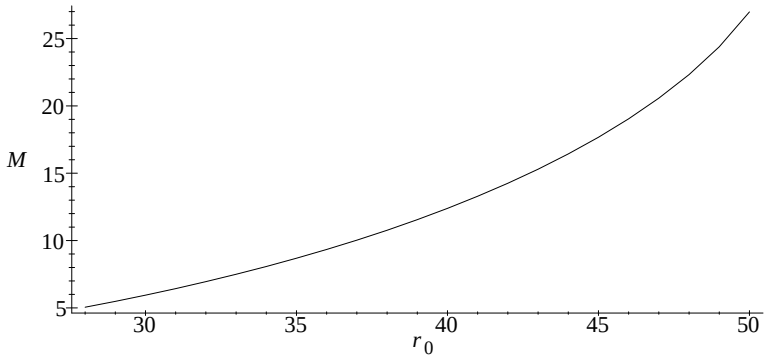

FIG. 8. The mass of the gravitational field versus the position r_0 of the pulse for massive NGT, where $A = 0.15$, and where $\sigma^2 = 1.6$ in the same units as r_0.

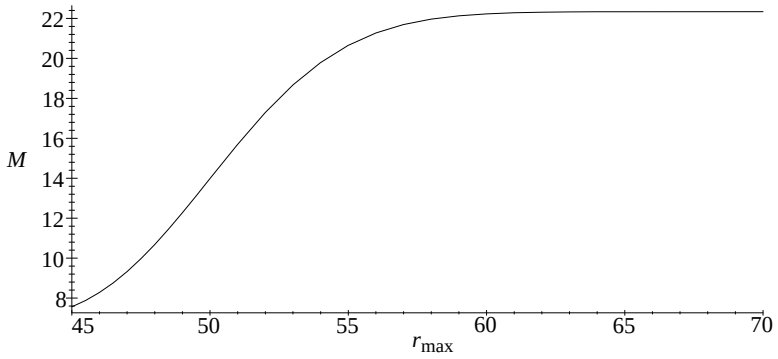

FIG. 9. The mass of the gravitational field of massles NGT as a function of the outer grid point, $r_{\max}$, for the initial conditions $\gamma^{11} = 1$, $\psi = A[r/r_0]^2 e^{-(r-r_0)^2/\sigma^2}$, and $j^2{}_3 = 0$, where $A = 0.7$, and with $\sigma = 10$ in units where $r_0 = 40$.

TABLE I. The residual Hamiltonian H_e and the ADM mass M as a function of the grid spacing Δr for massless NGT, for the initial data $\gamma^{11} = 1$ and $j^2{}_3 = 0$, with $\psi = A[r/r_0]^2 e^{-(r-r_0)^2/\sigma^2}$, where $A = 0.7$, and $r_0 = 40$ in units where $\sigma = 10$.

Δr	M	H_e
0.300	22.317	4.525×10^{-2}
0.150	22.334	1.129×10^{-2}
0.075	22.338	2.815×10^{-3}
0.030	22.340	4.554×10^{-4}
0.015	22.340	1.356×10^{-4}

asymptotic value of r_0 has not been reached. The reason for this is the same as mentioned above: the non-linear term in (2) begins to grow significantly, and the numerical code fails to find a solution. It is also interesting to note that when determining the bounds on the region of solvability for variations in σ (see Figure 5), (C4) seems to give particularly bad results, being off by a full order of magnitude. Although the predicted bound does not contradict the actual result, and no claim was made as to the accuracy of (C4), the reason for why there is such a large discrepancy is unknown at this time.

When calculating the ADM mass of a system, we must take into account the fact that our numerical grid is not of infinite size, whereas (8) implicitly assumes that the evaluation is performed at infinity. In Figure 9 we show how the ADM mass varies as the size of the grid is increased, for the initial data $\gamma^{11} = 1$ and $j^2{}_3 = 0$, with ψ given by (7), where $A = 0.7$, $r_0 = 40$ and $\sigma = 10$. As expected, the mass quickly converges to a definite value once the grid is sufficiently large. In our case, the mass has converged to within 0.01% when $r_{\max} = 70$. At this point, ψ has dropped to approximately 0.04% of its peak value. This justifies our choice of $r_{\max} = r_{\text{peak}} + 10\sigma$.

Finally, it is important to verify that the solution ϕ obtained by numerical means actually satisfies the Hamiltonian constraint, and if so, how well. This is somewhat of a thorny issue since, for a vacuum spacetime, the correct solution must make the Hamiltonian constraint vanish. It is therefore inheritly difficult to judge how well the solution satisfies this criterion without imposing some arbitrary precision level. One possibility, similar to that discussed by Bernstein *et. al.* (see Appendix A.3 in [42]) is to use the fact that in a non-vacuum spacetime, the Hamiltonian must be equated to the matter contributions: $\mathcal{H} = 2p\rho$. Thus, the error in the determination of ϕ can be viewed as a "matter contribution" to the right-hand side of the Hamiltonian constraint. Consequently, the mass of this contribution can be calculated and then compared with the known mass of the hypersurface, which then gives a measure of the precision of the solution.

In order to verify that the solution satisfies the Hamiltonian constraint to a sufficient degree, we calculate the

integral of absolute value of the Hamiltonian constraint:

$$H_{\rm e} = \int_\Sigma |\mathcal{H}|\, d^3x,$$

where the integration is performed over the volume of the slice Σ. We refer to H_e as the *residual Hamiltonian*, as it is a measure of that part of numerically-determined solution that violates the constraint. The residual Hamiltonian is then compared with the ADM mass M of the hypersurface. This process is repeated for successively smaller values of the grid spacing, until the ratio $H_{\rm e}/M$ is reduced to the desired level of precision. In Table I we list the results of such a calculation in the case of massless NGT for the initial data $\gamma^{11} = 1$ and $j^2{}_3 = 0$, with ψ given by (7) where $A = 0.7$, $r_0 = 40$, and $\sigma = 10$. The ADM mass and the residual Hamiltonian are given in the same units as Δr, the grid spacing. We see that as the grid spacing is reduced, the ADM mass converges to a definite value, in this case $M \approx 22.340$, and residual Hamiltonian decreases roughly as $(\Delta r)^2$. This is in keeping with the fact that our discretization of the Hamiltonian constraint was valid to second-order in the grid spacing.

V. CONCLUSIONS

We have described herein the foundation necessary for performing a thorough numerical study of spherically symmetric systems in NGT. By virtue of its construction, this formalism is not limited to a static gravitational field; this is particularly relevant for the spherically symmetric, Wyman sector initial data we have described in this work. In fact, the antisymmetric field variables are true dynamical degrees of freedom, not limited to being diffeomorphically related to a physically-equivalent static system by some analogue of Birkhoff's theorem.

We have demonstrated that the initial-value problem of NGT can be solved by numerical means, and that the solutions behave essentially as one would expect, based on a careful physical analysis of the situation, as described at the beginning of §IV. However, for a given initial data set, we cannot always solve the initial-value problem. We were able to place limits on the solvability of the Hamiltonian constraint for a particular distribution of the antisymmetric field variables. In itself, it is not particularly surprising that the initial-value problem cannot always be satisfied for all possible field configurations. What is surprising, however, is that certain seemingly acceptable configurations do not form a well-posed initial-value problem. In particular, for the case of the massive theory ($\mu \neq 0$), it was found that the antisymmetric field variables had to have particularly rapid fall-off in the asymptotic region in order to guarantee that the initial slice be asymptotically flat; otherwise, the final term in (2b), proportional to both $\sin\psi$ and ϕ^6, would feed back into the solution and destroy the desired asymptotic behaviour.

The behaviour of the ADM mass, or rather its NGT equivalent, was found to be a good indication of the solvability of the Hamiltonian constraint. Indeed, far from regions of unsolvability, the ADM mass was very small, corresponding to a weak field régime. On the other hand, near regions of unsolvability, the ADM mass became very large. But in the latter cases, the mass always began to display signs of reaching an asymptote. Again, this corresponds well with the underlying physical picture: a large mass cannot be obtained from an asymptotically flat spacetime, so demanding that the mass be large by increasing the size of the antisymmetric field variables causes us to step off the constraint surface, thereby violating the Hamiltonian constraint.

Of course, there remains much to be explored. For instance, we have not touched upon the topic of the Cauchy, or evolution problem in NGT. Once we are satisfied that a given field configuration properly satisfies the initial-value problem, we can then use the NGT evolution equations to determine the evolution of the system. The definition and existence of apparent horizons are also pivotal to the structure of NGT; this will be dealt with in a future publication.

Beyond this, we could modify the formalism (and hence the numerical code) to accommodate matter sources, thereby moving beyond the purely vacuum case that we have been considering here. Ideally, matter fields would be combined with an evolutionary approach, and we could make some headway into determining precisely what it is that happens in NGT when a stellar object expends its fuel and begins to collapse.

Perhaps the most critical aspect of NGT is that it remains as a candidate for a non-singular theory of gravitation. These claims are based on the study of a single, spherically symmetric, vacuum solution to the field equations of massless NGT (see [21] and [43]) as well as a certain amount of indirect theoretical evidence (see [44]). Meanwhile, some workers have claimed that NGT does exhibit the same singularity properties displayed in GR based on perturbative analyses of the field equations (see [45]). Ideally, we would prefer to consider initial data that describes a stellar model, essentially along the lines of the classic Oppenheimer-Snyder collapse problem in GR (see [46]), and "let the thing go". However, the mathematical difficulties involved in performing such feats has for some time relegated the topic to the area of pure speculation. Given the formalism we have outlined herein, this ideal is much more attainable than it once was.

ACKNOWLEDGMENTS

We would like to thank E. Seidel, and especially K. Camarda, for their help during the initial stages of this work, and N. Ó Murchadha for his help with some important theoretical details. We would also like to thank J. W. Moffat and P. Savaria for their many stimulating discussions. This work was partially funded by the Natural Sciences and Engineering Research Council of Canada. J. Légaré would like to thank the Walter C. Sumner Foundation for their funding of this research.

APPENDIX A: THE SPHERICALLY SYMMETRIC FIELD EQUATIONS OF NGT IN FIRST-ORDER FORM

A detailed description of the Hamiltonian form of NGT can be found in [23]. In this appendix, we give a brief overview of the reduction of these field equations for spherically symmetric systems. In particular, we will be considering exclusively the "Wyman sector" of NGT, also known as the electric sector (see [18–21]). The inverse fundamental tensor will therefore take the form $g^{-1} = e_\perp \otimes e_\perp - \gamma^{ab} e_a \otimes e_b$, where the basis vectors are defined by $N e_\perp = \partial_t - N^a \partial_a$ and $e_a = \partial_a$

The spherically symmetric form of a nonsymmetric tensor quantity can be found by a Killing vector analysis (see [23], p. 94). The spatial part of the inverse fundamental tensor and the extrinsic curvature are

$$\gamma^{ab} \to \begin{bmatrix} \gamma^{11} & 0 & 0 \\ 0 & \gamma^{22} & \gamma^{[23]}/\sin\theta \\ 0 & -\gamma^{[23]}/\sin\theta & \gamma^{22}/\sin^2\theta \end{bmatrix} \qquad \text{and} \qquad K_{ab} \to \begin{bmatrix} K_{11} & 0 & 0 \\ 0 & K_{22} & j_{[23]}\sin\theta \\ 0 & -j_{[23]}\sin\theta & K_{22}\sin^2\theta \end{bmatrix};$$

notice how we reserve the indexed symbols for the tensorial quantity with factors of $\sin\theta$ removed. The volume element is written

$$p\sin\theta = \sqrt{\gamma} = \sqrt{\det(|\gamma_{ab}|)} = (\gamma^{11}[(\gamma^{22})^2 + (\gamma^{[23]})^2])^{-1/2}\sin\theta.$$

The lapse function depends on the radial variable (and the time), $N = N(r,t)$, while the shift vector reduces to a single non-trivial component: $|N^a| \to [N^1, 0, 0]$. The vectors $|p^a|$ and $|\overline{W}_a|$ vanish by definition, being both native to the "Papapetrou" or magnetic sector of NGT. The non-zero components of the fundamental tensor are then

$$G_{11} = (\gamma^{11})^{-1}, \qquad G_{22} = \frac{\gamma^{22}}{(\gamma^{22})^2 + (\gamma^{[23]})^2}, \qquad \text{and} \quad G_{[23]} = -\frac{\gamma^{[23]}}{(\gamma^{22})^2 + (\gamma^{[23]})^2}.$$

We define the following:

$$K^1{}_1 = \gamma^{11} K_{11}, \qquad K^2{}_2 = \gamma^{22} K_{22} + \gamma^{[23]} j_{[23]}, \qquad \text{and} \quad j^2{}_3 = \gamma^{[23]} K_{22} - \gamma^{22} j_{[23]}.$$

For spherically symmetric Wyman sector initial data, the non-zero Lagrange multipliers and connection coefficients can be solved for, to wit: $a_1 = \partial_r[\ln N]$, and $\sigma^1 = \gamma^{11} a_1$, while

$$\Gamma^1_{11} = \tfrac{1}{2}\partial_r[\ln(p^2[(\gamma^{22})^2 + (\gamma^{[23]})^2])], \qquad \Gamma^2_{12} = \tfrac{1}{2}\partial_r[\ln(p^2\gamma^{11}[(\gamma^{22})^2 + (\gamma^{[23]})^2]^{1/2})],$$

and

$$\Gamma^1_{22} = -\gamma^{11}[G_{22}\Gamma^2_{12} - G_{[23]}\lambda^2_{13}].$$

The non-trivial components of the tensor $|\lambda^a_{bc}|$ are

$$\lambda^2_{13} = \tfrac{1}{2} G_{22}\gamma^{[23]}(\partial_r[\ln(p\gamma^{[23]})] - \partial_r[\ln(p\gamma^{22})]), \qquad \text{and} \quad \lambda^1_{23} = \gamma^{11}(G_{[23]}\Gamma^2_{12} + G_{22}\lambda^2_{13}).$$

Finally, the components of the NGT surface Ricci tensor are found using the connection coefficients and the components of $|\lambda^a_{bc}|$ given above:

$$R^{\mathrm{NS}(3)}_{11} = -2\partial_r[\Gamma^2_{12}] + 2\Gamma^2_{12}(\Gamma^1_{11} - \Gamma^2_{12}) - 2(\lambda^2_{13})^2, \qquad R^{\mathrm{NS}(3)}_{22} = \partial_r[\Gamma^1_{22}] + \Gamma^1_{22}\Gamma^1_{11} + 2\lambda^1_{23}\lambda^2_{13} + 1,$$

and

$$R^{\mathrm{NS}(3)}_{[23]} = \partial_r[\lambda^1_{23}] + \Gamma^1_{11}\lambda^1_{23} - 2\Gamma^1_{22}\lambda^2_{13}.$$

APPENDIX B: THE CONFORMALLY-TRANSFORMED FIELD EQUATIONS AND CONSTRAINTS FOR SPHERICALLY SYMMETRIC NGT

In order to approach the initial-value problem in NGT, in particular so as to study the solvability of the Hamiltonian constraint, we take the same route as in GR, which consists of conformally scaling the field variables by a factor ϕ, thereby transforming the Hamiltonian constraint into an equation for this conformal factor (see [47]). The variables $|\gamma_{ab}|$ and $|K_{ab}|$ are chosen to transform in some particular way, which then determines the transformation rules for the connection coefficients. Although this can be done in general in GR, the process is tantamount to inverting the compatibility condition, which in NGT is not nearly as trivial as in GR (see, for instance, [48,49]).

We choose $|\gamma_{ab}|$ and $|K_{ab}|$ to transform as $\gamma_{ab} \to \phi^4\gamma_{ab}$ and $K_{ab} \to \phi^{-2}K_{ab}$ (see [50]); from this we determine that $\gamma^{ab} \to \phi^{-4}\gamma^{ab}$ and $G_{ab} \to \phi^4 G_{ab}$, while $K^a{}_b \to \phi^{-6}K^a{}_b$ and $j^a{}_b \to \phi^{-6}j^a{}_b$. Note that we choose the transformation rule for the antisymmetric components of the fundamental tensor so that the determinant of the fundamental tensor transforms homogeneously in ϕ: $p \to \phi^6 p$. The non-trivial Lagrange multipliers are found to transform as $\sigma^1 \to \phi^{-4}\sigma^1$ and $a_1 \to a_1$, while the connection coefficients transform as

$$\Gamma^1_{11} \to \Gamma^1_{11} + 2\partial_r[\ln\phi], \qquad \Gamma^2_{12} \to \Gamma^2_{12} + 2\partial_r[\ln\phi], \qquad \text{and} \quad \Gamma^1_{22} \to \Gamma^1_{22} - 2\gamma^{11}G_{22}\partial_r[\ln\phi].$$

Finally, the components of the tensor $|\lambda^a_{bc}|$ transform as

$$\lambda^2_{13} \to \lambda^2_{13} \qquad \text{and} \qquad \lambda^1_{23} \to \lambda^1_{23} + 2\gamma^{11}G_{23}\partial_r[\ln\phi].$$

Despite its complexity, the transformation rule for the momentum constraint is relatively straightforward:

$$\begin{aligned}\mathcal{H}_1 \to \mathcal{H}_1 - 8p[K^1{}_1 + 2K^2{}_2]\partial_r[\ln\phi] = &-[K^1{}_1 + 2K^2{}_2]\partial_r[p] - K_{11}\partial_r[p\gamma^{11}] + 2K_{22}\partial_r[p\gamma^{22}] + 2j_{[23]}\partial_r[p\gamma^{[23]}] \\ &+ 4p\gamma^{22}\partial_r[K_{22}] + 4p\gamma^{[23]}\partial_r[j_{[23]}] - 8p[K^1{}_1 + 2K^2{}_2]\partial_r[\ln\phi] = 0.\end{aligned}$$

Meanwhile, the various terms in the Hamiltonian constraint transform differently, yielding

$$\begin{aligned}\mathcal{H} &= 8p\gamma^{11}\phi\partial_r^2[\phi] - 8p\phi\partial_r[\phi][\gamma^{11}\Gamma^1_{11} + 2\gamma^{22}\Gamma^1_{22} + 2\gamma^{[23]}\lambda^1_{[23]}] - p\phi^2 R^{\mathrm{NS}(3)} \\ &\quad - 2p\phi^{-6}[(K^2{}_2)^2 + 2K^1{}_1K^2{}_2 - (j^2{}_3)^2] - \tfrac{1}{4}\mu^2 p\phi^6\gamma^{[23]}G_{[23]} \\ &= 8p\phi\Delta_\gamma[\phi] - p\phi^2 R^{\mathrm{NS}(3)} - 2p\phi^{-6}[(K^2{}_2)^2 + 2K^1{}_1K^2{}_2 - (j^2{}_3)^2] - \tfrac{1}{4}\mu^2 p\phi^6\gamma^{[23]}G_{[23]} = 0,\end{aligned}$$

where in the last line, we have used the definition (C1) to write the Hamiltonian in the familiar Lichnerowicz form.

The evolution equations for the components of the fundamental tensor can be shown to transform in a somewhat simple manner:

$$\begin{aligned}\partial_t[\gamma^{11}] &= N^1\partial_r[\gamma^{11}] - 2\gamma^{11}\partial_r[N^1] - 4N^1\gamma^{11}\partial_r[\ln\phi] - 2N\phi^{-6}(\gamma^{11})^2K_{11}, \\ \partial_t[\gamma^{22}] &= \partial_r[N^1\gamma^{22}] - 4N^1\gamma^{22}\partial_r[\ln\phi] - 2N\phi^{-6}[(\gamma^{22})^2 + (\gamma^{[23]})^2]K_{22},\end{aligned}$$

and

$$\partial_t[\gamma^{[23]}] = \partial_r[N^1\gamma^{[23]}] - 4N^1\gamma^{[23]}\partial_r[\ln\phi] - 2N\phi^{-6}[(\gamma^{22})^2 + (\gamma^{[23]})^2]j_{23}.$$

The evolution equations for the components of the extrinsic curvature would be equally as simple, if not for the complicated transformation rule of the components of $\bar{\mathcal{Z}}_{ab}$; in fact, we find that

$$\begin{aligned}\partial_t[K_{11}] &= N^1\partial_r[K_{11}] + 2K_{11}\partial_r[N^1] - 2N^1K_{11}\partial_r[\ln\phi] - N\phi^2\bar{\mathcal{Z}}_{11} - \tfrac{1}{4}\mu^2 N\phi^6 G_{11}\gamma^{[23]}G_{[23]}, \\ \partial_t[K_{22}] &= N^1\partial_r[K_{22}] - 2N^1K_{22}\partial_r[\ln\phi] - N\phi^2\bar{\mathcal{Z}}_{22} + \tfrac{1}{4}\mu^2 N\phi^6 G_{22}\gamma^{[23]}G_{[23]},\end{aligned}$$

and

$$\partial_t[j_{[23]}] = N^1\partial_r[j_{[23]}] - 2N^1 j_{[23]}\partial_r[\ln\phi] - N\phi^2\bar{\mathcal{Z}}_{[23]} + \tfrac{1}{4}\mu^2 N\phi^6[\gamma^{[23]}(G_{22})^2 - G_{[23]}]$$

where

$$\begin{aligned}\bar{\mathcal{Z}}_{11} &= -4[\phi\partial_r^2[\phi] - (\partial_r[\phi])^2] + 2[\partial_r[\ln N] + 2\Gamma^1_{11} - 2\Gamma^2_{12}]\phi\partial_r[\phi] \\ &\quad + [R^{\mathrm{NS}(3)}_{11} + \partial_r[\ln N](\Gamma^1_{11} - \partial_r[\ln N]) - \partial_r^2[\ln N]]\phi^2 + [(K^1{}_1 + 2K^2{}_2) - 2K^1{}_1]K_{11}\phi^{-6}, \\ \bar{\mathcal{Z}}_{22} &= -2\gamma^{11}G_{22}[\phi\partial_r^2[\phi] + (\partial_r[\phi])^2] - 2[G_{22}\partial_r[p\gamma^{11}] - \Gamma^1_{22} + p\gamma^{11}G_{22}\partial_r[\ln N]]\phi\partial_r[\phi] \\ &\quad + [R^{\mathrm{NS}(3)}_{22} + \partial_r[\ln N]\Gamma^1_{22}]\phi^2 + [K^1{}_1K_{22} + 2j_{23}j^2{}_3]\phi^{-6},\end{aligned}$$

and

$$\begin{aligned}\bar{\mathcal{Z}}_{[23]} &= 2\gamma^{11}G_{[23]}[\phi\partial_r^2[\phi] + (\partial_r[\phi])^2] + [2G_{[23]}\partial_r[p\gamma^{11}] + 2\lambda^1_{[23]} + 2p\gamma^{11}G_{[23]}\partial_r[\ln N]]\phi\partial_r[\phi] \\ &\quad + [R^{\mathrm{NS}(3)}_{[23]} + \partial_r[\ln N]\lambda^1_{[23]}]\phi^2 + [K^1{}_1j_{[23]} - 2K_{22}j^2{}_3]\phi^{-6}.\end{aligned}$$

APPENDIX C: TWO CONSEQUENCES OF THE SOLVABILITY OF THE HAMILTONIAN CONSTRAINT FOR MASSLESS NGT IN SPHERICAL SYMMETRY FOR A MOMENT OF TIME-SYMMETRY

The Hamiltonian constraint of massless NGT for a moment of time-symmetry can be written in the form $8\phi\Delta_\gamma[\phi] = \phi^2 R^{\mathrm{NS}(3)}$, where the derivative operator $\Delta_\gamma[\,]$ is defined by

$$\Delta_\gamma[\phi] = \gamma^{11}\partial_r^2[\phi] - \partial_r[\phi](\gamma^{11}\Gamma^1_{11} + 2\gamma^{22}\Gamma^1_{22} + 2\gamma^{[23]}\lambda^1_{[23]}). \tag{C1}$$

We derive herein two criteria that are consequences of the existence of a function ϕ, solution of the Hamiltonian constraint of massless NGT, having the appropriate properties ($\phi > 0$ and $\phi - 1 \to 0$ as r^{-1} in the asymptotic region in order to guarantee finiteness of the energy.)[9]

Let f be a twice differentiable function with asymptotic fall-off. Since $\phi > 0$, then f can be written as the product $f = \phi u$, where u is also twice differentiable and has the same fall-off as f. Hence,

$$(\partial_r[f])^2 = \phi^2(\partial_r[u])^2 + 2\phi u\partial_r[\phi]\partial_r[u] + u^2(\partial_r[\phi])^2 = \phi^2(\partial_r[u])^2 + \phi\partial_r[\phi]\partial_r[u^2] + u^2(\partial_r[\phi])^2. \tag{C2}$$

Multiplying both sides by $p\gamma^{11}$ (to form a scalar density) and integrating gives

$$\int p\sin\theta\gamma^{11}(\partial_r[f])^2\,d^3x = \int \sin\theta(p\gamma^{11}\phi^2(\partial_r[u])^2 - \phi u^2\partial_r[p\gamma^{11}]\partial_r[\phi])\,d^3x = \int p\sin\theta(\gamma^{11}\phi^2(\partial_r[u])^2 - \phi u^2\Delta_\gamma[\phi])\,d^3x,$$

where the cross term $\phi\partial_r[\phi]\partial_r[u^2]$ in (C2) has been integrated by parts; the resulting surface terms vanish due to the fall-off of u and ϕ. Now, the first term on the right hand side is manifestly positive, so that we may conclude that

$$\int p\sin\theta\gamma^{11}(\partial_r[f])^2\,d^3x > -\int p\sin\theta u^2\phi\Delta_\gamma[\phi]\,d^3x.$$

However, assuming that ϕ is a solution of the Hamiltonian constraint and using the fact that $\phi u = f$, we may write

$$\int p\sin\theta\gamma^{11}(\partial_r[f])^2\,d^3x > -\frac{1}{8}\int p\sin\theta f^2 R^{\mathrm{NS}(3)}\,d^3x. \tag{C3}$$

This condition must be satisfied for all functions f with asymptotic fall-off. Alternately, if the Hamiltonian constraint admits a solution ϕ, then the NGT scalar curvature $R^{\mathrm{NS}(3)}$ is such that all functions f having asymptotic fall-off will satisfy (C3).

For any asymptotically flat Riemannian three-manifold, the Sobolev inequality [51] states that there exists a positive constant C such that[10]

$$\int p\sin\theta\gamma^{11}(\partial_r[\zeta])^2\,d^3x \geqslant C\Big[\int p\sin\theta\zeta^6\,d^3x\Big]^{1/3}$$

for any infinitely differentiable function ζ having compact support: $\zeta \in C_0^\infty$. For a flat manifold, the Sobolev constant is $C = \frac{3}{4}2^{2/3}\pi^{4/3}$. For a non-flat manifold, the value of C is most probably smaller [38]. Using the Sobolev inequality and the Hölder inequality (see [52], p. 52),

$$-\int p\sin\theta\zeta^2 R^{\mathrm{NS}(3)}\,d^3x \leqslant \Big[\int p\sin\theta\zeta^6\,d^3x\Big]^{1/3} \times \Big[\int p\sin\theta|R^{\mathrm{NS}(3)}|^{3/2}\,d^3x\Big]^{2/3},$$

we can transform (C3) into

$$\Big[\int p\sin\theta|R^{\mathrm{NS}(3)}|^{3/2}\,d^3x\Big]^{2/3} \leqslant 8C. \tag{C4}$$

---

[9] This proof is a slightly modified version of that which appears in [51]; the notation is similar, although it has been modified when necessary. It has been modified to fit your screen.

[10] Note that our constant C differs from that of Cantor and Brill; see, for instance, (10) in [51]. In fact, where we use C, they use C^{-1}.

The two inequalities (C3) and (C4) give qualitatively different results. The first of these is used to demonstrate that a data set *does not* support a solution of the Hamiltonian constraint, while the second is used to prove that a data set *does* support a solution of the Hamiltonian constraint.

---

[1] J. W. Moffat, *Phys. Rev. D* **19**, 3554 (1979).
[2] J. W. Moffat, *Found. Phys.* **14**, 1217 (1984).
[3] J. W. Moffat, in R. Mann and P. Wesson (eds.), *Gravitation: A Banff Summer Institute* (World Scientific, Singapore, 1991).
[4] J. W. Moffat, *Phys. Lett. B* **355**, 447 (1995).
[5] J. W. Moffat, *J. Math. Phys.* **36**, 3722 (1995).
[6] J. Légaré and J. W. Moffat, *Gen. Rel. Grav.* **27**, 761 (1995).
[7] J. W. Moffat, University of Toronto Preprint UTPT-96-05, gr-qc/9605016, (1996).
[8] A. Einstein, *Ann. Math.* **46**, 578 (1945).
[9] A. Einstein and E. G. Straus, *Ann. Math.* **47**, 731 (1946).
[10] A. Lichnerowicz, *J. Rat. Mech. and Anal.* **3**, 487 (1954).
[11] A. Lichnerowicz, *Théories Relativistes de la Gravitation et de l'Électromagnétisme: Relativité Générale et Théories Unitaires* (Masson et Cie., Paris, 1955).
[12] F. Maurer-Tison, *C. R. Acad. Sci.* **242**, 1127 (1956).
[13] V. Hlavatý, *Geometry of Einstein's Unified Field Theory* (P. Noordhoff Ltd., Groningen, 1958).
[14] F. Maurer-Tison, *Ann. scient. Éc. Norm. Sup.* **76**, 185 (1959).
[15] M. A. Tonnelat, *Einstein's Theory of Unified Fields* (Gordon Breach, New York, 1982).
[16] S. W. Hawking and G. F. R. Ellis, *The Large Scale Structure of Space-Time* (Cambridge University Press, Cambridge, 1973).
[17] M. A. Clayton, *J. Math. Phys.* **37**, 395 (1996).
[18] M. Wyman, *Can. J. Math.* **2**, 427 (1950).
[19] W. B. Bonnor, *Proc. Roy. Soc.* **209**, 353 (1951).
[20] J. R. Vanstone, *Can. J. Math.* **14**, 568 (1962).
[21] N. J. Cornish and J. W. Moffat, *Phys. Lett. B* **336**, 337 (1994).
[22] A. Papapetrou, *Proc. Roy. Soc. Irish Acad. Sci. A* **52**, 69 (1948).
[23] M. A. Clayton, *Massive Nonsymmetric Gravitational Theory: A Hamiltonian Approach*, Ph. D. dissertation, Department of Physics, University of Toronto, 1996.
[24] M. A. Clayton, to appear in *Int. J. Mod. Phys. D.*
[25] M. A. Clayton, *Class. Quant. Grav.* **13**, 2851 (1996).
[26] T. Damour, S. Deser, and J. McCarthy, *Phys. Rev. D* **45**, 3289 (1992).
[27] T. Damour, S. Deser, and J. McCarthy, *Phys. Rev. D* **47**, 1541 (1993).
[28] W. B. Bonnor, *Proc. R. Soc. A* **226**, 366 (1956).
[29] J. W. Moffat and I. Yu. Sokolov, *Phys. Lett. B* **378** 59 (1996).
[30] L. L. Smarr and J. W. York, *Phys. Rev. D* **17**, 2529 (1978).
[31] J. M. Stewart, in W. B. Bonnor, J. N. Islam, and M. A. H. MacCallum (eds.), *Classical General Relativity: Proceedings of the Conference on Classical (Non-Quantum) General Relativity, London, December 1983* (Cambridge University Press, Cambridge, 1984).
[32] D. H. Bernstein, D. W. Hobill, and L. L. Smarr, in C. R. Evans, L. S. Finn, and D. W. Hobill (eds.), *Frontiers in Numerical Relativity* (Cambridge University Press, Cambridge, 1989).
[33] P. Anninos, G. Daues, J. Massó, E. Seidel, and W.-M. Suen, *Phys. Rev. D* **51**, 5562 (1995).
[34] J. W. York and T. Piran, in R. A. Matzner and L. C. Shepley (eds.), *Spacetime Geometry: The Alfred Schild Lectures* (University of Texas Press, Austin, 1982).
[35] J. A. Wheeler, in B. DeWitt and C. DeWitt (eds.), *Relativity, Groups and Topology* (Gordon Breach, New York, 1964).
[36] N. Ó Murchadha and J. W. York, *Phys. Rev. D* **10**, 2345 (1974).
[37] N. Ó Murchadha, *Class. Quant. Grav.* **4**, 1609 (1987).
[38] N. Ó Murchadha, private communication.
[39] R. Arnowitt, S. Deser, and C. W. Misner, in L. Witten (ed.), *Gravitation: An Introduction to Current Research* (John Wiley and Sons, New York, 1962).
[40] M. A. Celia and W. G. Gray, *Numerical Methods for Differential Equations: Fundamental Concepts for Scientific and Engineering Applications* (Prentice Hall, Englewood Cliffs, 1992).
[41] L. Fox, *The Numerical Solution of Two-Point Boundary Problems in ODEs* (Dover Publications, New York, 1990).

[42] D. Bernstein, D. Hobill, E. Seidel, and L. Smarr, *Phys. Rev. D* **50**, 3760 (1994).
[43] N. J. Cornish, *Mod. Phys. Lett. A* **9**, 3629 (1994).
[44] J. W. Moffat, *J. Math. Phys.* **36**, 5897 (1995).
[45] L. Burko and A. Ori, *Phys. Rev. Lett.* **75**, 2455 (1995).
[46] J. R. Oppenheimer and H. Snyder, *Phys. Rev.* **56**, 455 (1939).
[47] A. Lichnerowicz, *J. Math. Pures Appl.* **23**, 37 (1944).
[48] M. A. Tonnelat, *J. Phys. Rad.* **12**, 81 (1951).
[49] M. A. Tonnelat, *J. Phys. Rad.* **16**, 21 (1955).
[50] J. York, in C. Evans, L. Finn, and D. Hobill (eds.), *Frontiers in Numerical Relativity* (Cambridge University Press, Cambridge, 1989).
[51] M. Cantor and D. Brill, *Composito Math.* **43**, 317 (1981).
[52] Y. Choquet-Bruhat, C. DeWitt-Morette, and M. Dillard-Bleick, *Analysis, Manifolds and Physics* (North-Holland Publishing Company, Amsterdam, 1977).